Further Evaluation of the RMMAC Method with Time-Varying Parameters

P. Rosa*, M. Athans*§, S. Fekri‡, C. Silvestre*
*Institute for Systems and Robotics/Instituto Superior Técnico, Lisbon, Portugal
§M. Athans is also Professor of EECS (emeritus), M.I.T., U.S.A.
‡Control and Instrumentation Research Group, University of Leicester, Leicester, UK
Emails: {prosa, athans, –, cjs}@isr.ist.utl.pt, sf111@le.ac.uk

***Abstract*— We demonstrate, using Monte-Carlo simulations, the superior performance of the "Robust Multiple-Model Adaptive Control (RMMAC)" method for different time-varying uncertain parameter waveforms, performance bandwidths and constant disturbance intensities using the test example designed and studied in Refs. [1] and [2]. We further show that the RMMAC RMS performance is just about 10-16% worse than that obtained from a system that has perfect model identification (which is unrealizable), while remaining vastly superior to the performance associated with the best robust non-adaptive design.**

***Index Terms*— Robust adaptive control, multiple-model adaptive control, time-varying parameters**

I. Introduction

The "Robust Multiple-Model Adaptive Control (RMMAC)" architecture, shown in Fig. 1, has been previously introduced and evaluated in Refs. [1-4]. We assume that the reader is familiar with the RMMAC methodology and, in particular, with the mass-spring-dashpot (MSD) test example presented in [1] and [2]. In our prior studies we stressed that the performance of any adaptive system must be evaluated not only for constant but unknown parameters but, also, for time-varying parameters which undergo slow or rapid time-variations. In this paper we use the same MSD example to evaluate the RMMAC performance for such time-variations for different intensities of unmeasurable plant disturbance.

In our previous studies, [1-5], the "goodness" of the RMMAC identification subsystem in the presence of time-varying parameters - which consists of the bank of the N Kalman filters (KFs) and of the "Posterior Probability Evaluator (PPE)" - was analysed by examination of the time-evolution of the posterior probabilities, $P_k(t)$, in Fig. 1. Often, there is a significant "transient identification time-interval" associated with the correct model identification by the associated posterior probability. It was not clear how such "model identification transients" impacted the RMMAC performance; in this paper, we quantify this issue by comparing the RMMAC performance to that associated with "Perfect Model Identification (PM.ID.)" using four different designs for the same MSD system. The details of this comparison are best explained by the examples considered.

This work was partially supported by Fundação para a Ciência e a Tecnologia (FCT), ISR/IST pluriannual funding, through the POS_Conhecimento Program that includes FEDER funds. The work of P. Rosa was supported by a PhD Student Grant from the FCT.

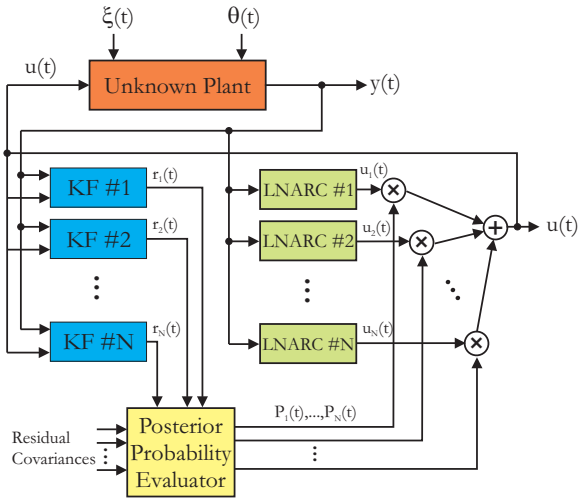

Fig. 1. The RMMAC architecture with N models

Two different cases are studied in this paper, both for the mass-spring-dashpot (MSD) system with uncertain spring constant and time-delay, shown in Fig. 2. First, a low frequency control bandwidth case is analyzed (previously designed in [1]), followed by a much harder control problem when the control bandwidth is higher (previously designed in [2]).

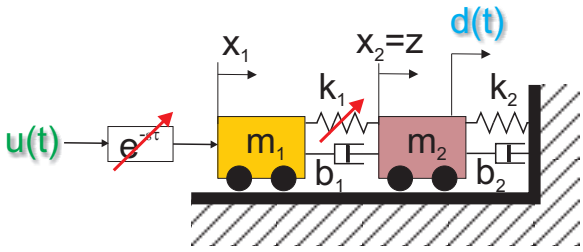

Fig. 2. MSD system with uncertain spring constant, k_1, and disturbances denoted by $d(t)$. $u(t)$ is the control input and $z(t)$ is the system output. τ is an uncertain time-delay bounded by $0 < \tau < 0.05s$, as in [1-2].

In order to evaluate the performance of the RMMAC methodology, two other types of controllers are considered, serving as benchmarks: the *best* global non-adaptive

robust controller (denoted by GNARC) and several local non-adaptive robust controllers (denoted by LNARCs) associated with the "perfect model identification scheme (PM.ID)". The GNARC determines the lower bound on robust performance in the absence of adaptive control. The LNARCs yield the best result one would expect since they correspond to perfect model identification. The performance of the RMMAC is within these two bounds.

Each dynamic model has associated one Kalman Filter, designed for a particular covariance matrix, $cov\,[\xi(t);\xi(\tau)] = E\{\xi(t)\xi'(\tau)\} = \Xi\delta(t-\tau)$, of the continuous-time zero-mean plant white noise $\xi(t)$, where Ξ is the plant-noise intensity matrix.

The disturbance force $d(t)$ shown in Fig. 2 is a stationary first-order (colored) stochastic process generated by driving a low-pass filter, with transfer function $W_d(s)$, with continuous-time white noise $\xi(t)$, with zero mean and intensity Ξ, according to eq. (1).

$$d(s) = \frac{\alpha}{s+\alpha}\xi(s) = W_d(s)\xi(s) \tag{1}$$

II. Low-Frequency Design (LFD) Simulations

Several simulations will now be presented for the LFD design, which uses α=0.1 rad/s. The RMMAC design for this LFD case is fully documented in [1] and [3] and all design choices and performance requirements remain the same. All the results were obtained with 5 Monte Carlo simulations, using τ = 0.01 s.

Four models (N=4) are required for the LFD RMMAC, so the performance of the RMMAC is not below 70% of the fixed nonadaptive robust controller (FNARC), as described in [1], [3] and [5]. The boundaries for the spring constant for each model are shown in Table I.

TABLE I
LFD RMMAC Model Definitions

Model	Spring Constant Interval
#1	Ω_1 = [1.02 1.75]
#2	Ω_2 = [0.64 1.02]
#3	Ω_3 = [0.4 0.64]
#4	Ω_4 = [0.25 0.4]

Case 1 (LFD): $\Xi = 1$, k_1 changing slowly

We start by analysing the behaviour of the RMMAC controller under the spring constant variation shown in Fig. 3. The spring constant is steady for 100 s. Then, it changes linearly until it is within the next model, keeping steady for another 100 s, and repeating the procedure. These changes take 50 s each, so the slope is in general not always the same. This is shown in Fig. 3, which also shows (using the dashed lines) the model boundaries as defined by Table I.

It is clear from Fig. 4 that during the k_1 slopes transitions, there is a transient associated with the identification process, taking about 50 s to enter a steady state for the associated posterior probabilities to correctly identify the model. Although the posterior probabilities in Fig. 4 follow roughly the transitions in waveform A, it is not clear how to judge the performance of the RMMAC system. For this reason we define the "Perfect Model Identification (PM.ID)" controller which simply generates the plant control $u(t)$ in Fig. 1 by switching in the correct LNARC at the instant that the waveform A in Fig. 3 crosses the model boundaries.

Figure 5 shows the results of 5 Monte Carlo simulations of the output $z(t)$ for the GNARC, RMMAC and PM.ID systems. It is evident from Fig. 5 that the RMMAC and PM.ID transients are very close; also the RMMAC performance is much better than that of the best non-adaptive design denoted by GNARC (as expected). These results imply that the "identification transients" of the posterior probabilities in Fig. 4 do not degrade the RMMAC performance significantly.

To further quantify these performance comparisons, we have computed the numerical values of the mean and RMS of the output $z(t)$ associated with Fig. 5. These are shown in Table II, for the PM.ID, RMMAC and GNARC designs, respectively. The last two columns of Table II show the following percentage comparisons

$$\begin{aligned} \%E &= \frac{RMMACvalue - PM.ID.value}{PM.ID.value} \\ \%F &= \frac{GNARCvalue - RMMACvalue}{RMMACvalue} \end{aligned} \tag{2}$$

Thus, %E measures the performance degradation of the RMMAC compared to that of the (unrealizable) instantaneous correct identification of the PM.ID. Similarly, %F measures the performance degradation of the non-adaptive GNARC design as compared to that of the RMMAC. From Table II we can see that the "imperfect RMMAC identification" results in only 10% RMS performance degradation.

TABLE II
Case 1 (LFD) RMS and mean values of $z(t)$ for $\Xi = 1$ and waveform A

	PM.ID	RMMAC	GNARC	%E	%F
Mean	1.73e-5	1.53e-5	1.16e-4	-11.7%	658.5%
RMS	3.20e-5	3.52e-5	2.61e-4	10.0%	642.7%

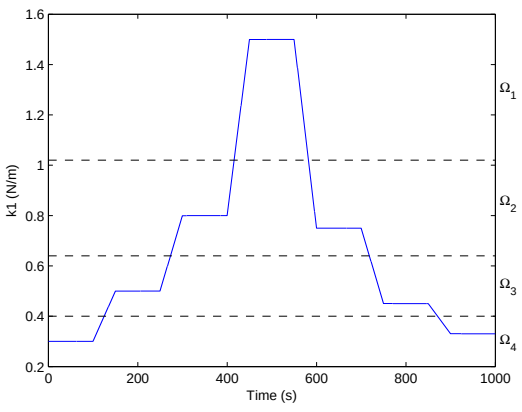

Fig. 3. Waveform A: Slowly time-varying spring constant, k_1

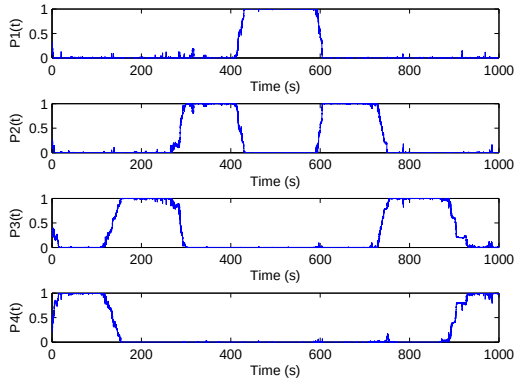

Fig. 4. Probability transients, $P_k(t)$, for $\Xi = 1$ and waveform A

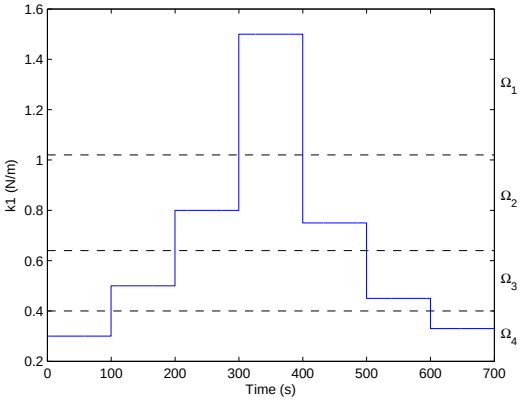

Fig. 6. Waveform B: Fast time-varying spring constant, k_1

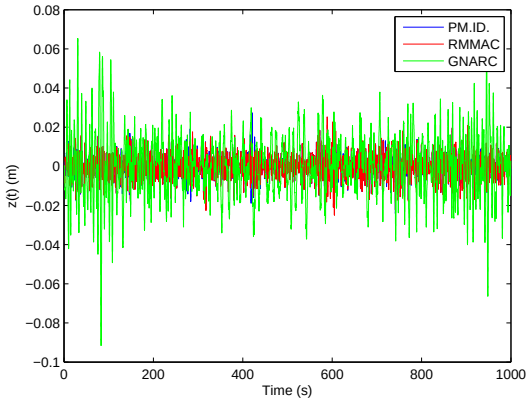

Fig. 5. Mass position, $z(t)$, for $\Xi = 1$ and waveform A

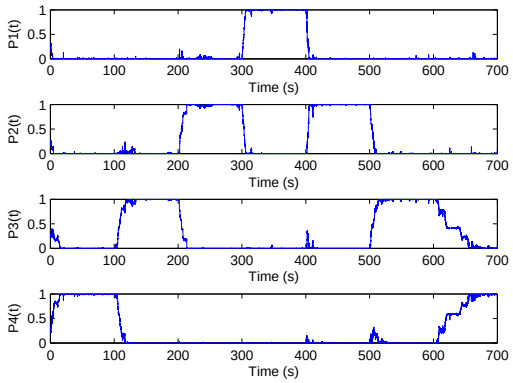

Fig. 7. Probability transients, $P_k(t)$, for $\Xi = 1$ and waveform B

Case 2 (LFD): $\Xi = 1$, k_1 with step changes

Next, a slightly different scenario is analyzed. The spring constant time variation is the staircase function shown in Fig. 6, which means that it stays constant for 100 s and then jumps to another constant value.

Figure 7 shows the posterior probabilities evolution. The identification process is now faster, taking only about 20 s to correctly identify the model at the most cases.

One might expect worse results when the spring changes in a staircase manner. In fact, the results remain almost unchanged for the RMMAC controller, as one can see from Table III. This result is more significant since GNARC performance is worse than that of the previous case.

TABLE III

CASE 2 (LFD) RMS AND MEAN VALUES OF $z(t)$ FOR $\Xi = 1$ AND WAVEFORM B

	PM.ID	RMMAC	GNARC	%E	%F
Mean	-9.16e-6	-1.06e-5	7.14e-5	15.6%	-774.4%
RMS	3.29e-5	3.67e-5	2.968e-004	11.5%	707.6%

Case 3 (LFD): $\Xi = 100$, k_1 changing slowly

In this experiment we increase the intensity matrix of the plant white noise, see eq. (1), to the value $\Xi = 100$. This causes the (unmeasurable) plant disturbances to be much larger; hence, one may expect that this may lead to a much more difficult identification and more significant degradation of the RMMAC performance. The KFs in the RMMAC architecture must be redesigned for this new intensity matrix; this was done in [1] and for this reason no further details are provided.

In this set of simulations we use the slow time-varying spring constant shown on Fig. 3, waveform A. It turns out that the evolution of the RMMAC posterior probabilities is almost identical to those shown in Fig. 4 and, hence, not shown here. There is an identification transient of about 50 s before the correct model is identified. The performance comparisons are illustrated in Fig. 8. Obviously, the RMS value of the mass position, $z(t)$, has increased (Table IV), since the disturbances power is also greater. Nonetheless, it is remarkable that the increase on the RMS is just about 3% more than in the previous case, summarized in Table II.

Case 4 (LFD): $\Xi = 100$, k_1 step changes

The results of using $\Xi = 100$ and changing the spring constant according to Fig. 6 are presented in Fig. 9 and in Table V. We do not show the evolution of the posterior probabilities; they are essentially the same as those shown in Fig. 7. The performance comparisons remain almost the same.

TABLE IV
CASE 3 (LFD) RMS AND MEAN VALUES OF $z(t)$ FOR $\Xi = 100$ AND WAVEFORM A

	PM.ID	RMMAC	GNARC	%E	% F
Mean	9.98e-5	5.99e-5	1.18e-3	-39.9%	1875.8%
RMS	2.87e-3	3.26e-3	2.55e-2	13.3%	682.1%

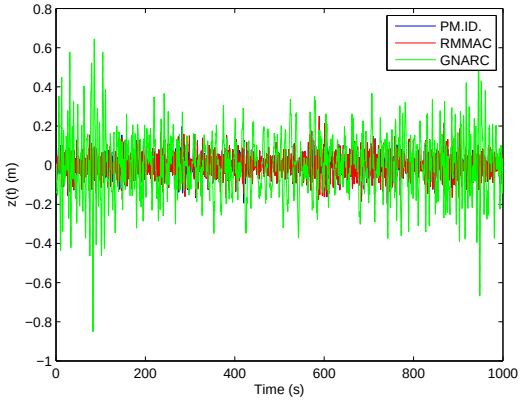

Fig. 8. Mass position, $z(t)$, for $\Xi = 100$ and waveform A

TABLE V
CASE 4 (LFD) RMS AND MEAN VALUES OF $z(t)$ FOR $\Xi = 100$ AND WAVEFORM B

	PM.ID	RMMAC	GNARC	%E	%F
Mean	-4.15e-5	-5.71e-5	9.02e-4	37.3%	-1681.7%
RMS	2.96e-3	3.34e-3	2.87e-2	12.7%	759.4%

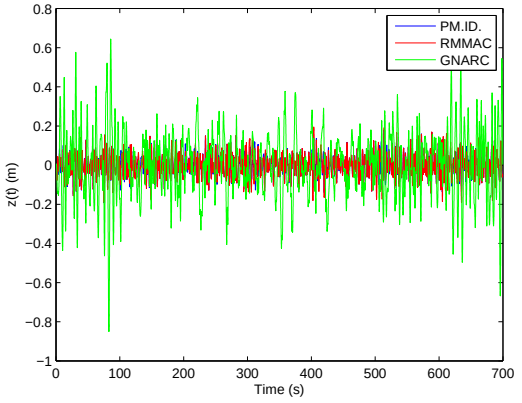

Fig. 9. Mass position, $z(t)$, for $\Xi = 100$ and waveform B

III. HIGH-FREQUENCY DESIGN SIMULATIONS

In this section we present similar performance comparisons to those in Section II using a different RMMAC design for the same MSD plant shown in Fig. 2. We refer to this set of results as the "High Frequency Design (HFD)" which is fully described in Refs [2] and [5]. The basic difference with the LFD design discussed above is that we use α = 3 rad/s in eq. (1). This means that the disturbance force $d(t)$ acting upon the MSD system has significant power over a much wider frequency range which strongly excites all the resonant modes of the MSD system. As described in full detail in [2] this requires a higher bandwidth design and corresponds to a much more challenging adaptive control problem.

The details of the HFD RMMAC design are fully described in [2] and are not repeated here. Based upon the posed adaptive performance specifications, [2], the RMMAC architecture of Fig. 1 requires N=7 models which are summarized in Table VI. As explained in Ref. [2], in this HFD case, the performance improvements of the RMMAC over the GNARC are much smaller than those possible in the LFD case. However, it is still important to quantify the RMMAC performance degradation as compared to that obtained by the "perfect model identification (PM.ID)".

TABLE VI
HFD RMMAC MODEL DEFINITIONS

Model	Spring Constant Interval
#1	Ω_1 = [1.4 1.75]
#2	Ω_2 = [1.11 1.4]
#3	Ω_3 = [0.85 1.11]
#4	Ω_4 = [0.65 0.85]
#5	Ω_5 = [0.49 0.65]
#6	Ω_6 = [0.35 0.49]
#7	Ω_7 = [0.25 0.35]

Case 5 (HFD): $\Xi = 1$, k_1 changing slowly

The spring constant time-evolution is depicted in Fig. 10. As seen from Table VII, the RMS value of the error is only about 12.5% above the one obtained wih a perfect identification process. It should be noted in Fig. 11 that the identification process is worse than the LFD case (see Fig 4). This means that in this case the identification of the system is harder. As discussed in [2], the larger the number of models the more difficult it is to resolve between adjacent models; however, the control probabilistic weighting inherent in the RMMAC architecture, generates good controls because the LNARC compensators for adjacent models are quite similar. This explains the modest performance deterioration noted in Table VII. The output transients are shown in Fig. 12. In summary, the RMS value of the error is similar to the LFD case, where the identification worked better. So, despite what might be expected, the poorer identification of the system did not result on significantly worse performance.

TABLE VII
CASE 5 (HFD) RMS AND MEAN VALUES OF $z(t)$ FOR $\Xi = 1$ AND $k1$ FOR WAVEFORM C

	PM.ID	RMMAC	GNARC	%E	%F
Mean	7.10e-3	8.35e-3	2.81e-2	17.6%	236.5%
RMS	9.84e-3	1.11e-2	6.13e-2	12.5%	453.5%

Case 6 (HFD): $\Xi = 1$, k_1 step changes

Similarly to what was done for the LFD case, we now consider the spring constant changing in a staircase manner, as depicted in Fig. 13. Table VIII shows the

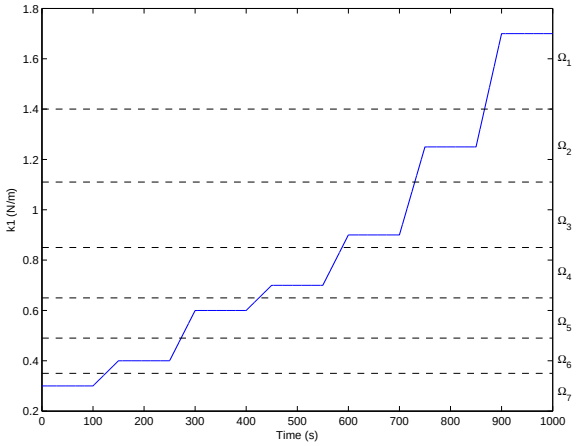

Fig. 10. Waveform C: Slowly time-varying spring constant, k_1

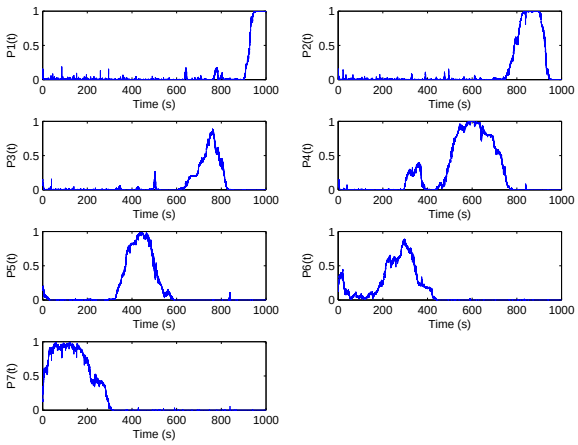

Fig. 11. Waveform C probability transients, $P_k(t)$, for $\Xi = 1$

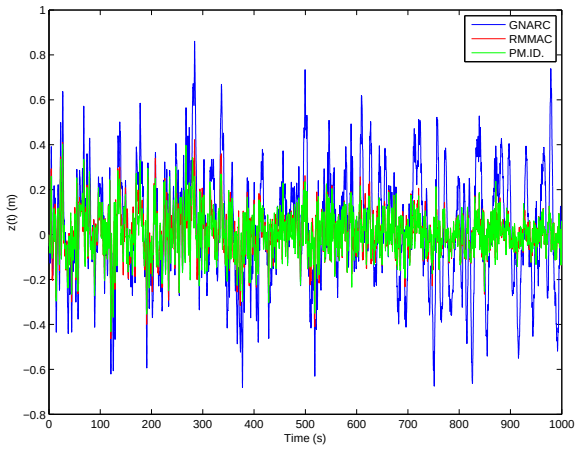

Fig. 12. Mass position, $z(t)$, for $\Xi = 1$ and waveform C used in HFD designs

results for this case, where one can see that the RMS value of $z(t)$ remains almost unchanged when compared to the previous example. This means that, for this problem, the absolute value of the uncertainty derivative does not significantly affect the results, as shown in Fig. 14. Once again, somewhat "confused" identification problems are observed (see Fig. 15), but the performance remains almost as good as in the previous case.

TABLE VIII
CASE 6 (HFD) RMS AND MEAN VALUES OF $z(t)$ FOR $\Xi = 1$ AND WAVEFORM D

	PM.ID	RMMAC	GNARC	%E	%F
Mean	1.96e-3	1.90e-3	1.58e-2	-3.1%	728.3%
RMS	1.04e-2	1.19e-2	5.97e-2	14.7%	401.9%

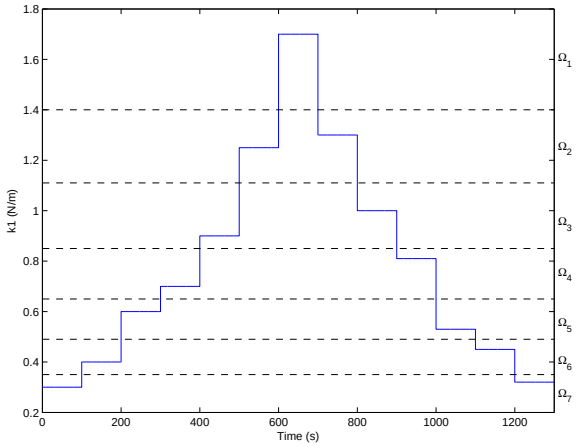

Fig. 13. Waveform D: Fast time-varying spring constant, k_1 (HFD)

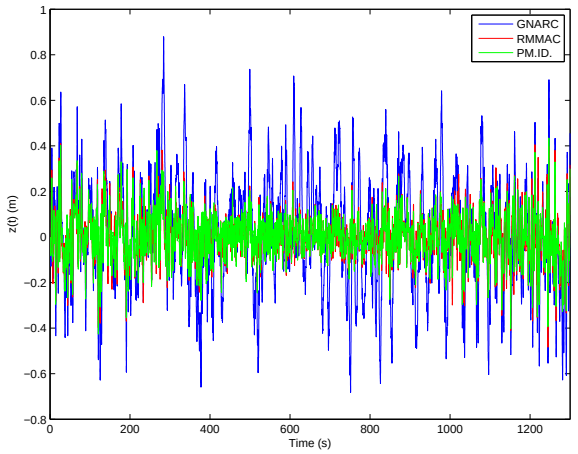

Fig. 14. Mass position, $z(t)$, for $\Xi = 1$ and waveform D

Case 7 (HFD): $\Xi = 100$, k_1 changing slowly

Here we use the time-varying k_1 given by Fig. 10. We also increase the intensity of the white noise so the disturbances have higher power. There are no significant differences between the resulting posterior probabilities from those shown in Fig. 11 and, hence, not shown. The increase on the RMS value of the output when comparing the RMMAC with the controller with perfect identification is about 14%, as shown on Table IX. From Fig. 16 it can be seen that the RMMAC behaves like the LNARC with PM.ID. when the spring constant stays level.

Case 8 (HFD): $\Xi = 100$, k_1 changing with steps

For these simulations, the $k_1(t)$ depicted in Fig. 13 is used. Table X presents the comparison between the

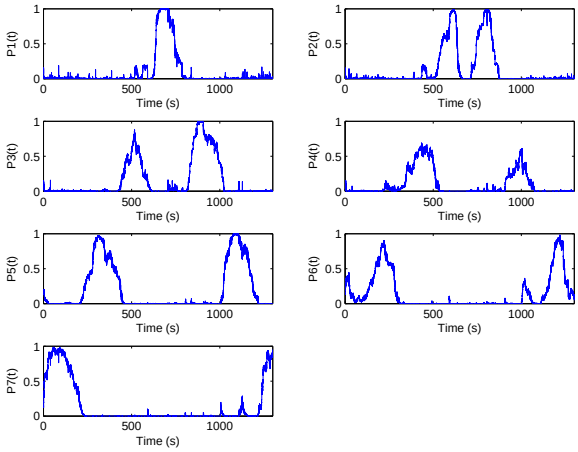

Fig. 15. Probability transients, $P_k(t)$, for $\Xi = 1$ and waveform D

TABLE IX
CASE 7 (HFD) RMS AND MEAN VALUES OF $z(t)$ FOR $\Xi = 100$ AND WAVEFORM C

	PM.ID	RMMAC	GNARC	%E	%F
Mean	7.10e-2	8.32e-2	2.81e-1	17.2%	237.3%
RMS	9.83e-1	1.12	6.12	13.6%	448.1%

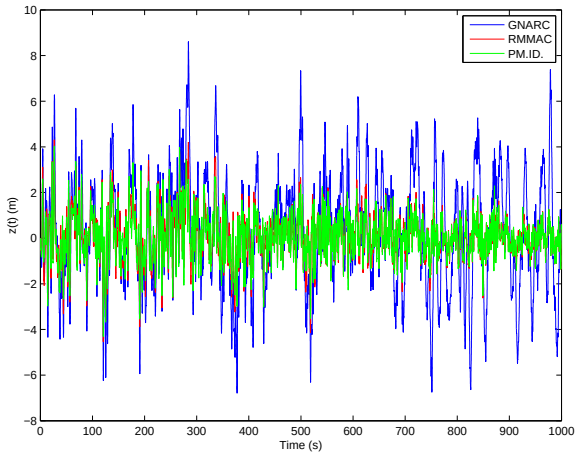

Fig. 16. Mass position, $z(t)$, for $\Xi = 100$ and waveform C

RMMAC and the benchmark controllers. We do not show the evolution of the posterior probabilities since they behave almost in an identical manner as those shown in Fig. 15. The output transients (not shown) look like those in Fig. 15, except for a scale change due to the higher disturbance intensity.

TABLE X
CASE 8 (HFD) RMS AND MEAN VALUES OF $z(t)$ FOR $\Xi = 100$ AND WAVEFORM D

	PM.ID	RMMAC	GNARC	%E	%F
Mean	1.93e-2	1.92e-2	1.57e-1	-0.3%	717.8%
RMS	1.04	1.208	5.97e	16.7%	393.9%

IV. CONCLUSIONS AND FUTURE WORK

We have demonstrated, using the specific MSD test example described in Refs. [1-3], that the RMMAC system significantly improves the performance of the best non-adaptive design (the GNARC system) for a variety of "slow" and "fast" variations of the uncertain spring constant, disturbance intensities and performance requirements. In this vein, the results presented herein further reinforce the conclusions related to the RMMAC methodology reached in our previous studies.

We have also focused upon the quality of the "model identification" process as exhibited by the time-evolution of the RMMAC posterior probabilities. As the uncertain parameter changes with time it induces a dynamic change of the true model. Ideally the posterior probabilities should instantaneously identify the correct model. However, a "learning transient" is inevitable. We have quantified the impact of this learning transient in the posterior probabilities by comparing the RMMAC performance (primarily using RMS errors) with that of a perfect "model identification (PM.ID.)" system; of course, such a PM.ID. system cannot be implemented. We have found that the RMMAC imperfect identification results only in a 10%-16% RMS performance degradation compared to the PM.ID. system. This small performance degradation is due to the fact that (a) the RMMAC controls are generated by "probabilistic averaging" [1-3], [5] and (b) the LNARC compensators used in the RMMAC architecture are quite similar for adjacent models, which account for the major model-learning transients of the RMMAC identification subsystem.

In a companion paper, Ref. [6], we evaluate the so-called RMMAC/XI architecture discussed in [1-3], [5] for the case that we have *simultaneous* time-variation of the uncertain parameter *and* the disturbance intensity.

REFERENCES

[1] S. Fekri, M. Athans, A. Pascoal, "Issues, progress and new results in robust adaptive control, " *Int. J. of Adaptive Control and Signal Processing*

[2] S. Fekri, M. Athans, A. Pascoal, "Robust multiple model adaptive control (RMMAC): A case study, " *Int. J. of Adaptive Control and Signal Processing*, 2006, in press

[3] M. Athans, S. Fekri, A. Pascoal, "Issues on robust adaptive feedback control," *Preprints of 16th IFAC World Congress*, pp. 9-39

[4] S. Fekri, M. Athans, A. Pascoal, "A two-input two-output robust multiple model adaptative control (RMMAC) case study," *American Control Conference*, Minneapolis, Minnesota, USA, June 2006.

[5] S. Fekri, "Robust adaptive MIMO control using multiple-model hypothesis testing and mixed-μ synthesis," Ph.D. dissertation, Instituto Superior Tecnico, Lisbon, Portugal, December 2005

[6] P. Rosa et al, "Evaluation of the RMMAC/XI Method with Time-Varying Parameters and Disturbance Statistics, MED07 (submitted)